RSC Advances

ROYAL SOCIETY OF CHEMISTRY

www.rsc.org/advances

Amperometric sensing of urea using edge activated Graphene Nanoplatelets

Vanish Kumar[a,b,*], Aditi Chopra[a], Shweta Arora[a], Shriniwas Yadav[a,b], Suresh Kumar[c], Inderpreet Kaur[a,b,*]

[a] Central Scientific Instruments Organisation (CSIR-CSIO), Sector-30C, Chandigarh, 160030, India.

[b] Academy of Scientific and Innovative Research (AcSIR), CSIR-CSIO, Sector-30C, Chandigarh, 160030, India.

[C] Department of Physics, University Institute of Engineering and Technology (UIET), Panjab University, Chandigarh, 160014.

Email address: inderpreety@yahoo.co.in, vanish.saini01@gmail.com

ABSTRACT

Sensing of urea is the key component in the diagnosis of kidney related diseases and milk adulteration. Till now the methods developed for urea sensing are not easy to perform, and very little attention has been paid to commercialization of such sensors. Herein, we first time report the low cost Graphene nanoplatelets (GNPlts) based sensing platform for urea. Specifically edge functionalized GNPlts are used for keeping graphitic activity of graphene planes intact. We have successfully sensed variable ranges of urea concentrations from 0.1-0.8mg/ml. The amperometeric characterization showed a linear variation in current as a function of urea concentration. The developed platform has a rapid response time of 15 sec with good sensitivity (33 μA (mg ml^{-1})$^{-1}$) and specificity. This developed nanoplatform could be highly beneficial for the development of ultrasensitive, disposable, routine use sensor for urea.

Keywords: Graphene nanoplatelets, Amperometric sensing, Nanoprobe, Urease, Urea.

1. Introduction

Urea is an organic compound present in milk and urine of mammals and is synthesized from the metabolism of nitrogen containing compounds like proteins, etc. Presence of high concentration of urea in the body is a major indicator of kidney failure. On the other hand, urea is also a main adulterant of milk and any change in the urea concentration (lower or higher) in milk is a symbol of adulteration [1,2,3]. The allowable range of urea in milk is 0.2 to 0.4 mg/ml and any

deviation from this concentration reports the milk as adulterated [4]. Therefore, the development of urea sensing platform with good accuracy and precision is of utmost importance. Till now enzyme coupled, Infrared (IR) spectroscopy, pH, amperometric, flow injection and fiber optics based methods are developed for urea sensing but all these techniques are not easy to perform in meager instrumental facilities [5,6,7]. At the same time, commercial viability of these techniques is also very low. With the increasing commercialization of milk products, parameterization and standardization of milk is essential, thus there is a need to develop efficient urea sensors. In addition, urea sensing is also needed for the diagnosis of kidney related diseases. Exploiting new materials like graphene, which has been reported highly efficient for ballistic conductance and amperometeric sensing can give a unique platform for sensitive and specific sensors.

This article is focused on sensing of urea by employing urease conjugated graphene nanoplatelets (GNPlts). Like graphene, GNPlts are also extraordinary in their chemical and physical properties, but have short stacks of sheets and platelets like morphology. GNPlts show superiority over other porous materials as the surface area of GNPlts is very less affected by the pore distribution [8,9,10]. Rather, porosity provides high surface for electrolyte movement even on agglomeration as the ions still manage to migrate through interstices to access the GNPlts surface [11 , 12] . This property of GNPlts makes them excellent candidate for development of electrochemical sensors. The edge functionalization of GNPlts can further improve sensing strategy because it preserves the graphitic nature of basal plane and due to repulsion among functional groups on the edges they tends to self-exfoliate, resulting in high quality GNPlts films [13]. Such sensing platforms made up of GNPlts used in this work will be further beneficial for the economy and commercialization.

Urease is an enzyme, which causes hydrolysis of urea. The hydrolysis results in generation of ammonium (NH_4^+) and carbonic ions (HCO_3^-) [14,15].

$$NH_2CONH_2 + H^+ + 2H_2O \xrightarrow{\textbf{Urease}} 2NH_4^+ + HCO_3^-$$

The main purpose of this research is to efficiently sense the ions, produced during hydrolysis of urea. The GNPlts were edge functionalized with urease to improve sensitivity. Conjugation of urease was done via EDC-NHS coupling and the activity of conjugated GNPlts-urease is tested by conducting indothymol and pH based study. The developed platform has been transferred on

the working region of carbon nanotubes coated Screen Printed Electrodes (SPE). This GNPlts/CNT-SPE platform can easily and efficiently detect the generation of ions, which ultimately leads to urea estimation present in samples. It was observed that when a voltage sweep of 0V to +1V is applied across the platform, it gave a residual current at 0V on interactions of urea and urease. This residual current is explored to measure the estimation of urea.

2. Materials and Methods

GNPlts were purchased from XG sciences, (Michigan) having typical surface area of 50-80 m^2/g with average particle diameter of 25 microns and bulk density of 0.03 to 0.1 g/cc. CNT-SPE were purchased from DropSens, India. EDC and NHS were purchased from Sigma-Aldrich. Other chemicals like H_2SO_4, HNO_3, and HCl were purchased from Merck & Co., Inc, (India). All the materials used in the present study were of analytical grade.

Bioconjugation of urease: Edge functionalized GNPlts were obtained by controlled oxidation of GNPlts. GNPlts were mixed in a solution of H_2SO_4:HNO_3 (3:1) and ultrasonicated continuously for one hour. After obtaining the uniform dispersion, the sample is placed in an ice bath and 2ml of 10 M HCl was added drop wise. The sample was again subjected to sonication for 30 min and left for 4 hours at room temperature [16]. The solution obtained was filtered through hydrophilic PTFE filter membrane (0.2 μm pore size) and washed repeatedly with deionized (DI) water to remove excess acid. Carboxylated GNPlts were dried and dispersed in aqueous solution for urease bio-conjugation. The urease was attached to GNPlts with the help of EDC-NHS cross linker. EDC is a zero length cross linker which facilitates the amide bond formation between amine and carboxyl functionalized species. NHS increases the bonding efficiency (10 to 20 fold) [17]. GNPlts (1mg/ml), Urease (1mg/ml) were mixed with 0.05 M of EDC and 5 mM of NHS at room temperature for 2 hour and then stored at 4°C overnight. The overnight storage hydrolyzes unreacted EDC and causes loss of activity [18]. The unreacted enzyme and chemicals were removed by vacuum filtration with repeated washing. Further, the conjugate was mixed with DI water and ultra-centrifuged at 15,000 rpm leading to complete removal of excess unconjugated materials. At last, urease conjugated GNPlts were immobilized on CNT-SPEs for urea sensing. Different concentrations of urea ranging from 0.1 mg/ml to 0.8 mg/ml were prepared for conducting experiments. Keithley's 4200 SCS system was used to investigate the current-voltage (IV) characteristics of the sensing probe during the hydrolysis of urea. Furthermore, conjugation

of urease was confirmed by FTIR (Thermo Scientific NICOLET iS10), Raman (Renishaw inVia Raman microscope) and UV-Vis (Varian-5000 UV-VIS spectrophotometer) spectroscopy, whereas the edge functionalization (immobilization of urease) was ascertained by EDS (Energy-dispersive X-ray spectroscopy) attached with FE-SEM (Hitachi S-4800).

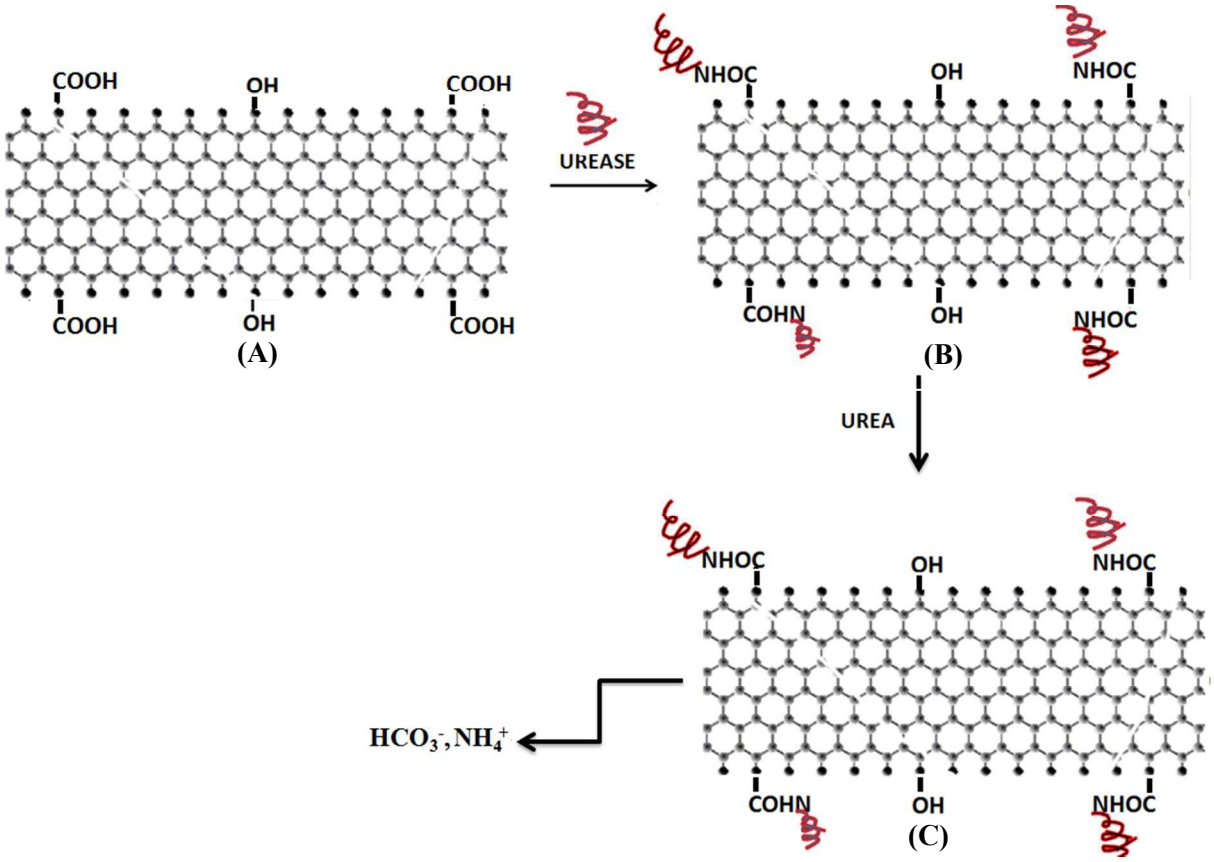

Fig.1. Schematic representation of (A) Edge carboxylated GNPlts, (B) Graphene urease conjugate, (C) Generation of ions after the addition of urea.

3. Results and discussion

The main focus of this article is on efficient sensing of urea with urease edge modified GNPlts. In this study, we have conjugated urease with GNPlts. Sensing of urea is done using this conjugate immobilized on CNT-SPE and employed for urea sensing (Fig. 1).

3.1 FTIR characterization

FTIR spectrum of GNPlts (Fig. 2) shows weak peaks at 3420 and 2920 cm^{-1} which are due to O-H and graphitic skeletal respectively. In case of carboxylated graphene, various peaks of oxygen containing groups were observed. The intensity of 3420 cm^{-1} peak found to be

increased to a great extent due to generation of –OH groups on GNPlts surface. The peak at 1736 cm^{-1} is due to C=O stretching of –COOH group present on the edges of GNPlts. The peak at 1635 cm^{-1} may be attributed to O-H deformation [19,20].The peak observed at 1365 cm^{-1} is due to C–O-H vibrations present in carboxylic group [21]. The above results confirmed that oxygen containing groups were generated on the GNPlts surface after treatment with acids. However, untreated GNPlts also have few peaks which are responsible for oxygen containing groups, but the intensity of these peaks is very less. The oxygen containing groups in untreated GNPlts may be due to air oxidation or presence of moisture on GNPlts. The carboxylic groups generated on the surface of GNPlts were utilized for amide bonding with amine group of urease. In case of urease conjugated GNPlts, the prominent peaks of amide bond were observed at 1650 cm^{-1} (amide C=O stretch) and 3440 cm^{-1} (amide N-H stretch) [22,23].

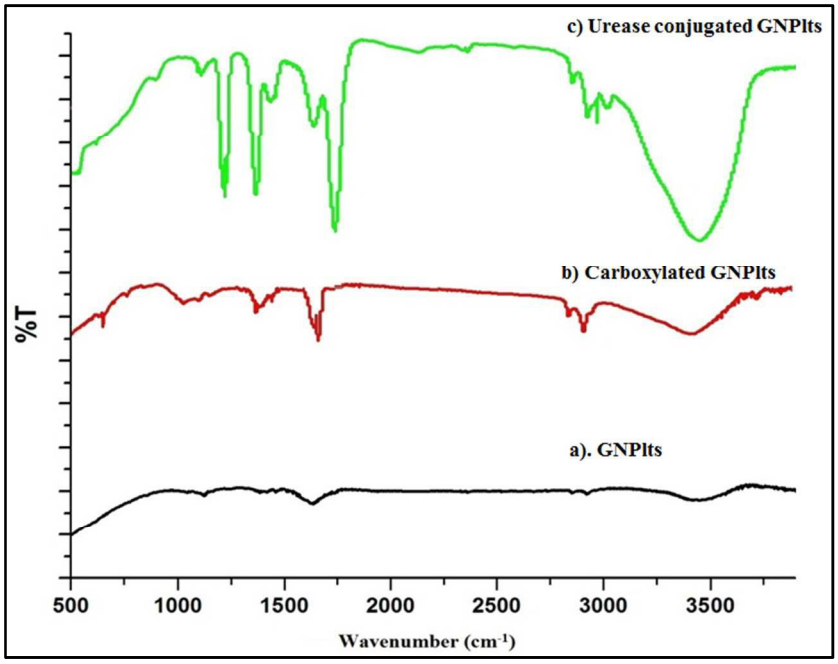

Fig.2. FTIR spectra for a) GNPlts, b) Carboxylated GNPlts, and c) Urease conjugated GNPlts.

3.2 Bioconjugation studies of GNPlts with urease

The bioconjugation of GNPlts with urease is confirmed by means of UV-Vis and Raman spectroscopies. As shown in Fig. 3, the conjugate formation resulted in UV absorption at 278 nm, which is due to the presence of urease enzyme in the conjugate. Urease contain some aromatic amino acids (Trp, Tyr and Phe) which shows π-π* transition, hence resulting in UV absorption at 278 nm. The peak at 278 nm shows blue shift with hyperchromatic effect after

conjugation of urease with GNPlts (i.e., it shifts to 272 nm). This blue shift may be attributed to the interaction between urease and GNPlts [24].

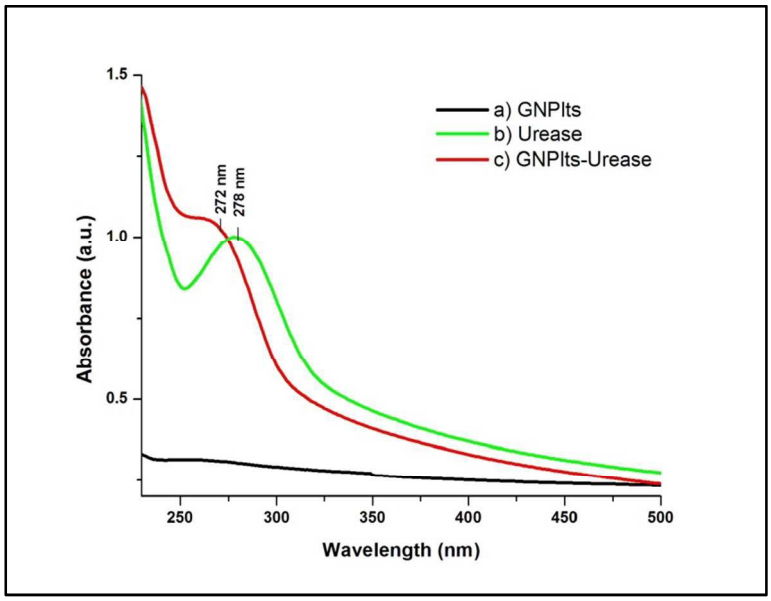

Fig.3. UV-VIS spectra for a) GNPlts, b) Urease and c) GNPlts-Uresase conjugate.

Fig. 4 represents the Raman spectra of GNPlts, carboxylated GNPlts and Urease conjugated GNPlts. Raman spectroscopy plays an important role in the characterization of carbon based materials. The main peaks arises in the carbonic samples are D peak (~1350 cm^{-1}), G peak (~1580cm^{-1}) and 2D peak (~2700 cm^{-1}). Raman spectroscopy potentially differentiates between sp^2 carbons from other carbonic structures [25,26,27,28]. Raman spectra obtained at each step majorly of three samples- pristine GNPlts, carboxylated GNPlts and urease conjugated GNPlts. The spectra revealed very interesting peaks and alteration in intensities (Fig. 4). Raman spectra of all the three samples is mainly consisted of D (1355 cm^{-1}), G (1584 cm^{-1}) and 2D (2710 cm^{-1}) band. The relative intensities of D, G and 2D-Bands were altered after functionalization. Oxidation of GNPlts causes generation of defects and results in skeletal deformation of sp^2 structure which give rise to increase in the relative intensity of D-band after carboxylation. The increase in the intensity of D-band is proportional to the deformation in the sp^2 skeletal, which ultimately confirms the functionalization. The extent of functionalization was further confirmed by I_D/I_G ratio. The I_D/I_G ratio for GNPlts, carboxylated GNPlts and urease functionalized GNPlts were found to be 0.0167, 0.23, and 0.35 respectively. The pristine GNPlts have very less I_D/I_G ratio due to presence of very few defects in sp^2 skeletal. In case of carboxylated GNPlts this ratio

increased sharply due to generation of numerous defects during acid treatment. Upon conjugation of urease a little increase of 0.12 was observed in I_D/I_G ratio. This increase is mainly due to further functionalization of GNPlts and shielding of sp^2 signals due to wrapping/covering of GNPlts surface with urease [29].

It is further to mention that the edges of GNPlts are very fragile and whenever a chemical treatment is given it is likely to attack the edges. 2D peak in Raman is the result of interlayer interaction of GNPlts and after getting functional groups at the edges, these GNPlts have more tendency to self exfoliate leading to more intense peak at 2700 cm^{-1}.[30]

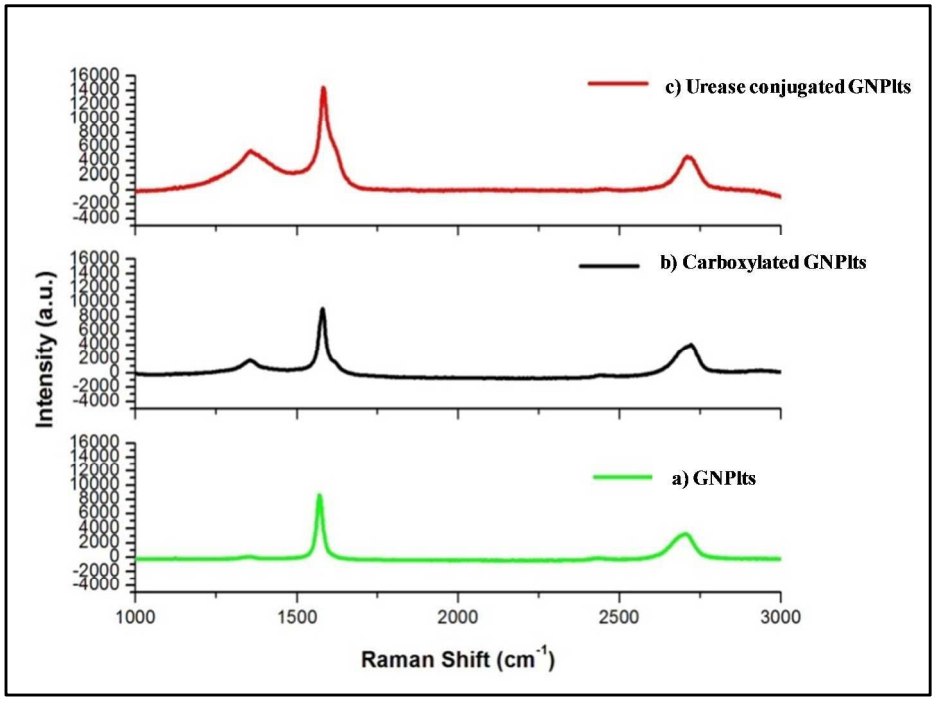

Fig.4. Raman spectra of a) GNPlts, b) Carboxylated GNPlts, c) GNPlts-Urease.

3.3 FE-SEM and EDS Analysis

Surface morphology of bare CNT-SPE and GNPlts immobilised CNT-SPE (working electrode) is shown in Fig. 5a & b. FE-SEM and EDS analysis of GNPlts conjugated with urease is shown in Fig. 5c & d. The Microscopic analysis clearly shows GNPlts have an average length of 10 to 15 µm. On the sheet points 1, 2, 3 and 5 are specifically chosen on the central/Basal region of graphene while the points 4, 6, 7, 8 and 9 are taken on the edges of the graphene (Fig.

5c). The elemental data is taken at all the points through EDS as tabulated (Fig. 5d). On comparing the data collected from edges and basal points, it is clear that the edges of nanoplatelets have the peaks for carbon, nitrogen and sulfur, while the central region of the nanoplatelet has only carbonic content. The main reason for presence of nitrogen and sulfur in GNPlts is urease as it is composed of nitrogen rich amino acids. The presence of nitrogen at the GNPlts edges confirms edge functionalization with urease.

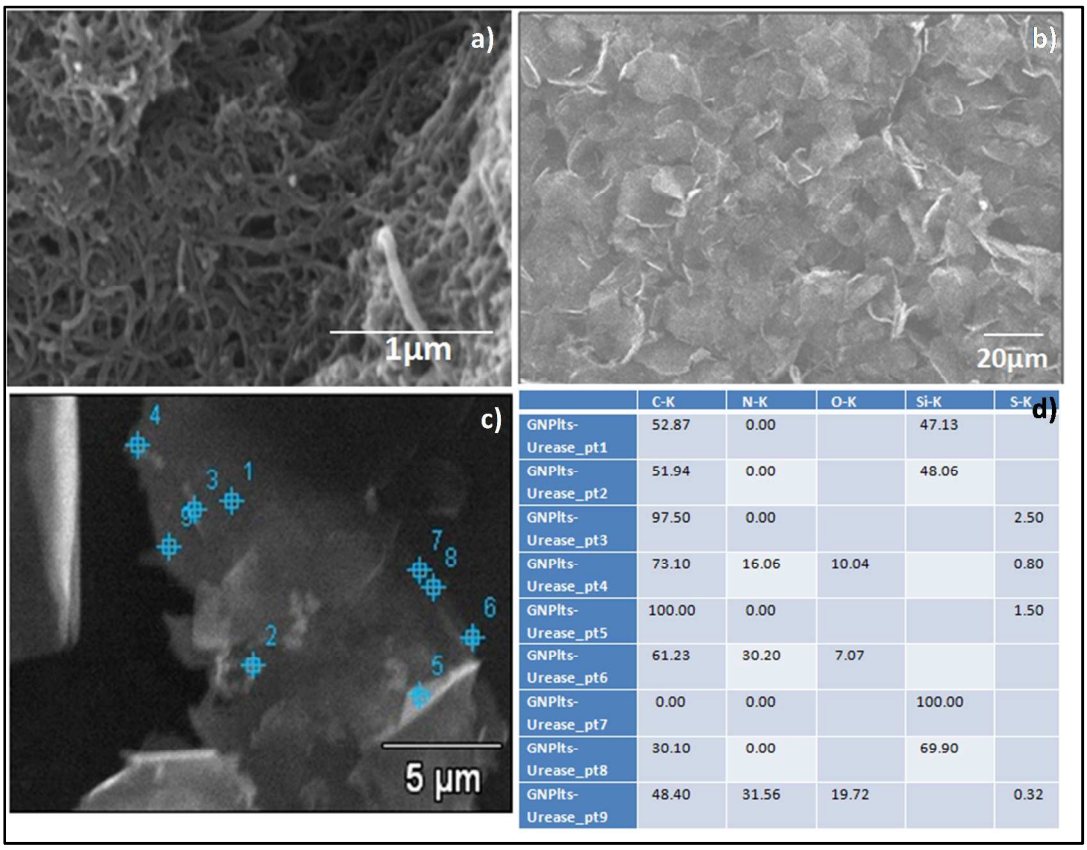

	C-K	N-K	O-K	Si-K	S-K
GNPlts-Urease_pt1	52.87	0.00		47.13	
GNPlts-Urease_pt2	51.94	0.00		48.06	
GNPlts-Urease_pt3	97.50	0.00			2.50
GNPlts-Urease_pt4	73.10	16.06	10.04		0.80
GNPlts-Urease_pt5	100.00	0.00			1.50
GNPlts-Urease_pt6	61.23	30.20	7.07		
GNPlts-Urease_pt7	0.00	0.00		100.00	
GNPlts-Urease_pt8	30.10	0.00		69.90	
GNPlts-Urease_pt9	48.40	31.56	19.72		0.32

Fig.5. a) FE-SEM micrograph of CNT-SPE, b) FE-SEM micrograph of GNPlts dropcasted CNT-SPE, c) and d) FE-SEM micrograph and EDS analysis (at different regions) of urease conjugated GNPlts. The points in SEM micrograph shown is chosen for EDS analysis. The EDS analysis shown (table) the weight % of different atom present on urease conjugated GNPlts. The edges of nanoplatelets have the peaks for carbon, nitrogen and sulfur, while the central region of the nanoplatelet has only carbonic content.

3.4 Sensing of Urea

The urease conjugated GNPlts were immobilized on CNT-SPE by simple dropcasting method. The prepared substrate is used for sensing of urea. As the edges are active for hydrolysis of Urea, therefore addition of urea leads to the generation of ammonium and carbonic ions,

which are responsible for variation in electron transport parameters. The most important electron transport parameters here are conductivity, mobility of charge carriers and shift in Dirac point of Graphene leading to current at 0V. On addition of different concentrations of urea, the conductivity of the urease conjugated GNPlts immobilized on CNT-SPE platform is measured. All the measurements are linear and ohmic in nature. From the graph, we can conclude that there is a considerable variation in the I-V characteristics with varying urea concentration.

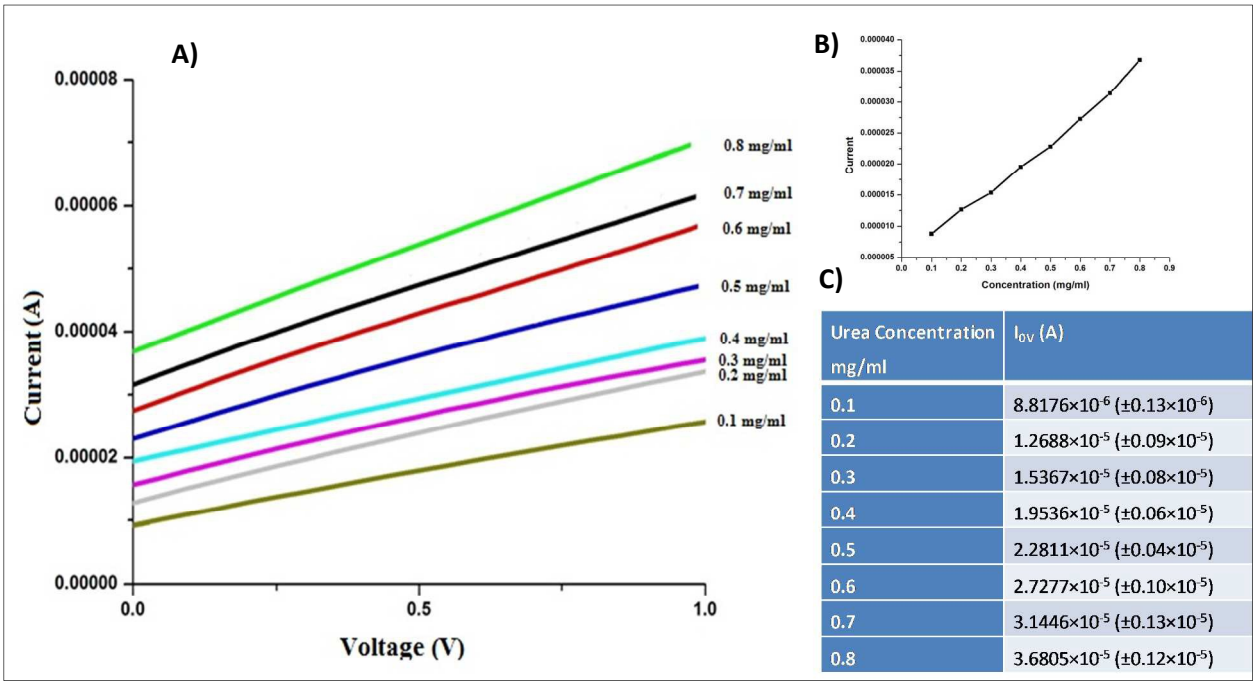

Urea Concentration mg/ml	I_{0V} (A)
0.1	8.8176×10^{-6} ($\pm0.13\times10^{-6}$)
0.2	1.2688×10^{-5} ($\pm0.09\times10^{-5}$)
0.3	1.5367×10^{-5} ($\pm0.08\times10^{-5}$)
0.4	1.9536×10^{-5} ($\pm0.06\times10^{-5}$)
0.5	2.2811×10^{-5} ($\pm0.04\times10^{-5}$)
0.6	2.7277×10^{-5} ($\pm0.10\times10^{-5}$)
0.7	3.1446×10^{-5} ($\pm0.13\times10^{-5}$)
0.8	3.6805×10^{-5} ($\pm0.12\times10^{-5}$)

Fig.6. Sensing of urea by using urease conjugated GNPlts and CNT-SPE. A) IV-characteristics of urease conjugated GNPlts at different concentration of urea B) Urea concentration (mg/mL) vs average current (Ampere) produced during sensing of urea C) Table showing average current produced upon addition of urea on proposed platform.

As any straight line graph IV can be understood by the equation

$$I= (1/R)\ V+I_{0V}$$

Here I is the measured current and V is the applied voltage, 1/R is the slope of the IV curve and I_{0V} is the net current at 0 volt as shown in Fig. 6. There is an insignificant increase in the slope with increasing concentrations of urea. I_{0V} is the measure of conductivity due to the ions adhered on the graphene substrate. When Urea interacts with Urease, both positive and negative charge

carriers are generated. The conductivity is the net resultant of charge carriers generated and adhered on the surface of GNPlts.

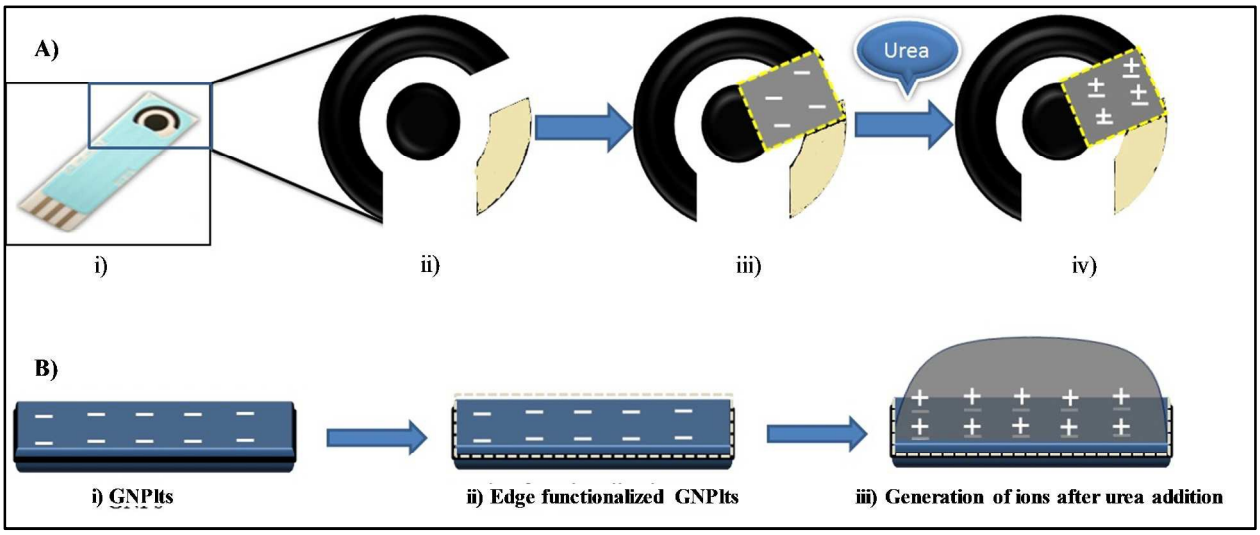

Fig.7. Accmulation of ions after urea hydroysis creating electrostatic layer A.i) Screen printed electrodes, ii) enlarged view of working area, iii) dropcasting of edge functionalized GNPlts at working area of SPE (edges are represented by yellow dots), iv) Generation and accumulation of ions after addition of urea, B.i) pristine GNPlts, ii) Edge functionalized GNPlts, iii) Generation and accumulation of ions on the GNPlts surface.

Since graphene is rich in electronic charges on the surface, the electrostatic layers or kind of gating region is generated by the surface potential at the graphene-liquid interface at the edges (Fig. 7). When the negative surface charge which is screened by ions attracts mobile positive charges to the graphene-liquid interface, the negative surface potential is formed on the surface. These positive charges are both positive charges (holes) in the graphene and positive ions in interface liquid. As the concentration of ions increases, more and more surface charges get screened, leading to affect the mobility of charge carriers [31, 32]. When the potential is applied across the graphene substrate, the ions in close proximity to the graphene can contribute to Coulomb scattering. Coulomb scattering due to charged impurities/residues adsorbed on the graphene surface and Coulomb scattering of graphene charge carriers by charged ions can be the dominant scattering mechanisms, hence a consistent small increase in conductivity for the conjugate is observed [33].

As observed in Fig. 6, the curves are not passing through the origin; instead of 0V the curves are showing a definite positive value of current. The adhered ions/ionic contamination on the graphene substrate lead to shift in dirac point of the graphene, giving rise to conductivity at 0V which could be considered as the measure for urea ions and can be a parameter for sensing [31].

This positive value of current (I_{0V}) is due to the positive shift in dirac point during hydrolysis of urea. As the concentration of urea increases, the urease cause generation of more ions, which resulted in increased I_{0V}. When I_{0V} is plotted w.r.t. concentration, an almost linear graph with average slope 3.3 x 10^{-5}A/(mg ml^{-1}). This is a direct measure of sensitivity of the developed platform for urea. The results indicate a clear variation in the value of I_{0V} even with minute change in the urea concentration. We successfully sense urea from concentration range of 0.1 mg/mL to 0.8 mg/mL with a response time of 15 seconds by using this nanohybrid platform.The sensitivity of the system is quite high and may work well for urea adulteration range present in milk. In order to study the effect of interfering molecules (like calcium phosphate, calcium citrate, and magnesium citrate [34, 35]), control experiments were conducted and we found a negligible change in I_{0V}. Therefore, it can be used as an efficient sensor to monitor the concentration of urea.

Conclusion

Graphene and graphene based nanomaterials has arisen as the forefront of research in electrochemical sensing due to its promising properties, especially the unique electrical and surface modification features. Sensitivity of electron transport in graphene to the presence of ions in solution may lead to a new paradigm of electrochemical sensors and biosensors.

Sensing of urea using nanohybrid platforms especially GNPlts could be a very efficient technique for specific and sensitive detection of urea. The conjugate was immobilized on CNT-SPE and utilized for amperometeric sensing. GNPlts/CNT-SPE hybrid successfully achieved good linearity with very less response time for urea sensing. This platform will be helpful in determining urea adulteration and diagnosis of kidney related diseases. The developed platform is reusable and can be used around 20 times without any significant change in results when stored in 0.02M potassium phosphate buffer of pH 7 at 4ºC after proper washing.

Such devices are stable over days of measurements and exhibit small change in mobility of charge carriers on cycling multiple times. Research on such sensing techniques could be highly beneficial for the development of advance, ultrasensitive, disposable, portable and routine use sensors for other bioanalytes finding application in various areas.

Acknowledgement

The authors acknowledge the funding support from *Council of Scientific and Industrial Research- Senior Research Fellowship (*CSIR-SRF), Nanotechnology: Impact on Safety, Health and Environment Program (CSIR-NANOSHE), and academic support from *Central Scientific Instruments Organization* (CSIR-CSIO), Academy of Scientific and Innovative Research (AcSIR). We also acknowledge other group members at CSIO, especially Sukhbir Singh and for their valuable suggestions and inputs.

References

1 T. W. Meyer, M.D., and T. H. Hostetter, M.D., N. Engl. J. Med., 2007, 13, 1316.
2 M. M. Paradkar, R. S. Singhal and P. R. Kulkarni, Int. J. D. Techol., 2000, 53, 87.
3 PFA (1996) The Prevention of Food Adulteration Act 1954 (Act No. 37 of 1954) with the prevention of food adulteration rules, 1955 and notifications. Allahabad: Law Publishers (India).
4 C. Bastin, L. Laloux, A. Gillon, F. Miglior, H. Soyeurt, H. Hammami, C. Bertozzi, and N. Gengler, J. Dairy Sci., 2009, 92, 3529.
5 A. F. Li, J. H. Wang, F. W. and Y. B. Jiang, Chem. Soc. Rev., 2010, 39, 3729.
6 P. Bhatia, B. D. Gupta, Sensors Actuat B- Chem., 2012, 161, 434.
7 M. S. Anský, A. Pizzariello, S. S. Anská, S. Miertuš, Anal. Chim. Acta, 2000, 415, 151.
8 J. Shen, Y. Hu, M. Shi, X. Lu, C. Qin, C. Li, and M. Ye, Chem. Mater., 2009, 21, 3514.
9 http://xgsciences.com/wp-content/uploads/2012/09/10-15-13_xGNPlts-H_Data-Sheet.pdf (retrieved on 10/07/2014)
10 J. Han, L. L. Zhang, S. Lee, J. Oh, K. S. Lee, J. R. Potts, J. Ji, X. Zhao, R. S. Ruoff, and S. Park, ACSNANO, 2013, 7, 19.
11 H. Kim, H. D. Lim, S. W. Kim, J. Hong, D. H. Seo, D. C. Kim, S. Jeon, S. Park and K. Kang, Sci. Rep., 2013, 3, 15061.
12 M. D. Stoller, S. Park, Z.Yanwu, J. An, and R. S. Ruoff, Nano Lett., 2008, 8, 3498.

13 I. Y. Jeon, Y. R. Shin, G. J. Sohn, H. J. Choi, S. Y. Bae, J. Mahmood, S. M. Jung, J. M. Seo, M. J. Kim, D. W. Chang, L. Dai, and J. B. Baekm, PNAS, 2012, 109, 5588.
14 J.K. Fawcett and J.E. Scott, J. Clin. PathoL, 1960, 13, 156.
15 T. Osaka, S. Komaba, M. Seyama, and K. Tanabe, Sensors Actuat B 1996, 36, 463.
16 G. Wang, J. Yang, J. Park, X. Gou, B. Wang, H. Liu, and J. Yao, J. Phys. Chem. C, 2008, 112, 8192.
17 S. Kumar, H. Kaur, H. Kaur, I. Kaur, K. Dharamvir, and L. M. Bharadwaj, 2012, 47, 1489.
18 S. Wang, N. Mamedova, N. A. Kotov, W. Chen, and J. Studer, Nano Lett., 2002, 2, 817.
19 Y. X. Ma, Y. F. Li, G. H. Zhao, L. Q. Yang, J. Z. Wang, X. Shan , and X. Yan, Carbon, 2012, 50, 2976.
20 T. Lin, J. Chen, H. Bi, D. Wan, F. Huang, X. Xie and M. Jiang, J. Mater. Chem. A, 2013, 1, 500.
21 Y. Si and E. T. Samulski, Nano Lett., 2008, 8, 6, 1679.
22 H. Zhou, X. Wang, P. Yu, X. Chena and L. Mao, Analyst, 2012, 137, 305.
23 Q. Hong, C. Rogero, J. H. Lakey, B. A. Connolly, A. Houltona and B. R. Horrocks, Analyst, 2009, 134, 593.
24 W. Y. Qing , Z. H. Mei, Spectrochim. Acta Mol. Biomol. Spectros., 2012, 96, 352.
25 R.P. Vidano, and D.B. Fischbach, Solid State Commun., 1981, 39, 341.
26 F. Tuinstra and J. L. Koenig, J. Chem. phys, 1970, 53, 1126.
27 A. C. Ferrari, J. C. Meyer, V. Scardaci, C. Casiraghi, M. Lazzeri, F. Mauri, S. Piscanec, D. Jiang, K. S. Novoselov, S. Roth, and A. K. Geim, Phys. Rev. Lett., 2006, 97, 187401.
28 M. S. Dresselhaus, A. Jorio, M. Hofmann, G. Dresselhaus, and R. Saito, Nano Lett. 2010, 10, 751.
29 V. Georgakilas, M. Otyepka, A. B. Bourlinos,V. Chandra, N. Kim, K. C. Kemp, P. Hobza, R. Zboril, and K. S. Kim, Chem. Rev., 2012, 112, 6156.
30 A. C. Ferrari, J. C. Meyer, V. Scardaci, C. Casiraghi, M. Lazzeri, F. Mauri, S. Piscanec, D. Jiang, K. S. Novoselov, S. Roth, and A. K. Geim, Phys. Rev. Lett., 2006, 97, 187401.
31 Y. Y. Wang and P. J. Burke, Appl. Phys. Lett., 2013, 103, 052103.
32 J. Yin, X. Li, J. Yu, Z. Zhang, J. Zhou and W. Guo, Nat. nanotechnol., 2014, 9, 378.
33 A. K. M. Newaz, Y. S. Puzyrev, B. Wang, S. T. Pantelides and K. I. Bolotin, Nat. commun., 2012, 3, 734.
34 Š. Zamberlin, N. Antunac, J. Havranek, D. Samaržija, Mljekarstvo, 2012, 62, 111.
35 F. Gaucheron, Reprod. Nutr. Dev., 2005, 45, 473.

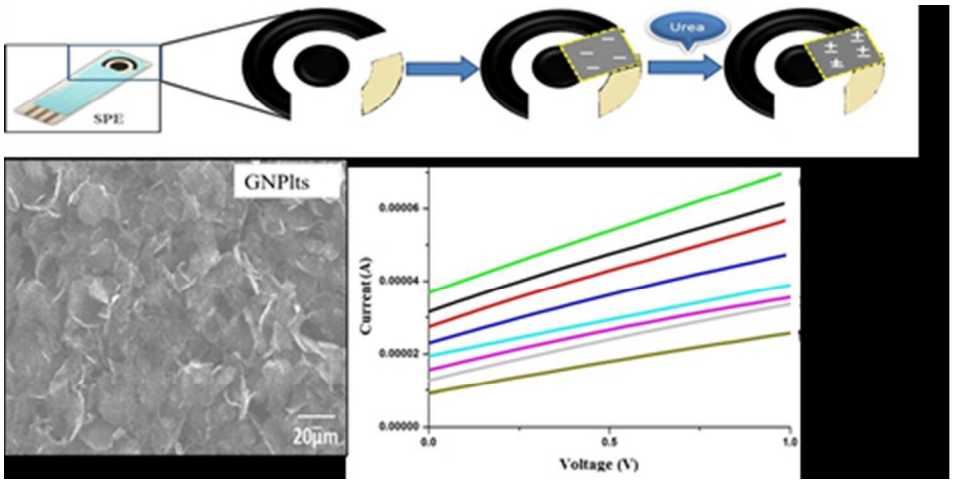

79x39mm (150 x 150 DPI)

In this study, we demonstrate efficient amperometric sensing of urea using graphene nanoplatelets.